ID

Coating of Sandblasted and Acid-Etched Dental Implants With Tantalum Using Vacuum Plasma Spraying

Xian Zhou, MD,* Xiulian Hu, DMD,† and Ye Lin, DMD‡

Although dental implants have become common prosthetics for missing teeth, the need for improved success rates and less complications has received increasing attention. Titanium (Ti) and its alloys are widely used as biomaterials in dentistry because of their excellent biocompatibility. However, the inherent surface bioinertness of Ti and its alloys hinders osseointegration between the implant and surrounding tissues.[1] Various methods including grit blasting, acid etching, coating, and electrochemical anodization as well as bioactive methods have been developed to modify the surface of Ti dental implants.[2–6] However, improved osseointegration is difficult to achieve. Even bioactive surface modifications do not always result in improved osseointegration. In addition, inflammation of soft and hard tissues around the implant caused by oral microflora persists. Periimplantitis is considered one of the main risk factors affecting the long-term survival rate of implants. Similar to periodontitis, this condition

Purpose: The objective was to prepare tantalum (Ta)-coated sandblasted and acid-etched (SLA) dental implants using vacuum plasma spraying (VPS) and to analyze their morphologies.

Materials and Methods: Twelve SLA implants were coated with Ta using VPS. The topographies of the coatings and Ta/SLA surface interfaces were examined using scanning electron microscopy. The thickness at 4 locations for 6 Ta-coated and 6 uncoated SLA implants and pore sizes of the neck, central, and root areas of Ta-coated implants were measured. SPSS v20.0 was used for statistical analysis.

Results: The Ta coatings were rough and consisted of pitted structures with various pore sizes; no cracks were observed. The Ta/SLA surface interface was tightly bonded. The 95% confidence interval of the Ta coating thickness was (114.0759, 129.3574). The maximal pore diameter was concentrated at 200 to 400 nm.

Conclusion: SLA dental implants were successfully coated with Ta using VPS. The nanoporous structure of these implants may facilitate osseointegration compared with uncoated SLA implants. (Implant Dent 2018;27: 202–208)

Key Words: morphology, coating thickness, bonding strength, scanning electron microscopy

is commonly caused by the attachment of bacterial plaque and a host response, resulting in bone resorption and even implant loss. A recent review summarized strategies for improving the antimicrobial functionalization of dental implants.[7] However, most of these strategies have only been tested *in vitro* under static conditions. The exploration of novel types of dental implants with excellent osteogenetic and antibacterial properties is of current interest.

Tantalum (Ta) is a rare metal that has attracted increased attention in implant dentistry because of its high corrosion resistance and excellent biocompatibility. A bacterial adhesion assay revealed lower bacterial adhesion of pure Ta compared with commonly used biomaterials in orthopedic implants.[8] The antibacterial activity of Ta has also been reported in other studies.[9,10] Moreover, previous studies have demonstrated the excellent biological performance of Ta with a porous structure[11–14] and even its predictable dental treatment outcomes.[15–18] For decades, Ta has been applied in orthopedics as a load-bearing metal[19–21]; however, the difficulty in manipulating solid Ta has limited its application. Attempts have been made to develop an open-cell porous biomaterial with a structure similar to trabecular bone, known as porous Ta trabecular metal (PTTM).[22] This material is fabricated on a foam-like vitreous carbon scaffold

*Master Degree Candidate, Department of Oral and Maxillofacial Surgery, Peking University School and Hospital of Stomatology, Beijing, China.
†Associate Professor, Department of Oral Implantology, Peking University School and Hospital of Stomatology, Beijing, China.
‡Professor, Department of Oral Implantology, Peking University School and Hospital of Stomatology, Beijing, China.

Reprint requests and correspondence to: Xiulian Hu, DMD, Department of Oral Implantology, Peking University School and Hospital of Stomatology, No. 22 Zhongguancun South Avenue, Haidian District, Beijing 100081, China, Phone: 86-10- 82195344, Fax: 86-10-62173402, E-mail: Sunhu33@163.com

using chemical vapor diffusion with hydrogen and chlorine gases.[23] PTTM-enhanced Ti dental implants have been designed and introduced[15,16,24] with PTTM material in the middle part of the implant, such as the Tapered Screw-Vent Implant produced by Zimmer Dental Inc., Carlsbad, CA. Its trabecular bone structure provides an enhanced surface for osseointegration. However, little is known about its biological reactions in the complex oral environment, and the relatively high cost and production difficulties limit its wide application.

Vacuum plasma spraying (VPS) is a relatively economical method for fabricating porous coatings in an atmosphere with very high melting temperatures. Studies have demonstrated that the preparation of porous metal structures using VPS is a promising strategy for bone regeneration. Tang et al[25] successfully fabricated porous Ta coatings on Ti substrates using VPS. These porous Ta coatings enhanced the osteogenic differentiation and bone regeneration of bone marrow stromal cells. A hydroxyapatite–silver coating on Ti implants was also prepared using this technique.[26] These findings indicate that VPS may be applicable for the fabrication of porous Ta coatings for dental implants.

In this study, we aimed to prepare porous Ta coatings on sandblasted and acid-etched (SLA) dental implants using VPS. The initially rough surface of the SLA implants was expected to enhance the bonding strength of the interface. Experiments were performed to investigate the morphological characteristics of the Ta-coated SLA surfaces compared with uncoated SLA samples. This part of study is to prepare for subsequently analyzing the effect of these coatings on osseointegration and antibacterial activity in the animal experiment.

MATERIALS AND METHODS

In this study, SLA implants were coated with Ta using VPS. The initial microstructures of the Ta coating surfaces without histologic staining were characterized using scanning electron microscopy (SEM; Hitachi S-4800, Tokyo, Japan).

Sample Preparation

Materials. The SLA implants were designed and manufactured by Weihai WEGO Jericom Biomaterials Co., Ltd. as substrates for the preparation of the Ta-coated implants. The implants had slightly tapered bodies with an outer diameter of 4 mm and a length of 8 mm (Fig. 1).

Ta metal powders (purity 99.9%; Zhuzhou Jiabang Refractory Metal Co., Ltd., Zhuzhou, China) with particle sizes ranging from 5 to 15 μm were used.

Experimental Equipment

A VPS system (Sulzer Metco, Winterthur, Switzerland) was used for fabrication of the Ta coatings with a spraying distance of 270 mm. Table 1 lists the spraying parameters used to prepare the Ta coatings. SEM (Hitachi S-4800, Tokyo, Japan) was used to examine the morphology and determine the thickness of the Ta coatings.

SEM Examination

The initial surfaces of the Ta-SLA implants were examined using SEM at varying magnifications. Sites were randomly selected from the neck, central, and root areas of the Ta-coated samples to determine the morphological differences of the different regions.

Twelve samples (6 Ta-coated and 6 uncoated SLA implants) were selected to determine the thickness of the Ta coating layer. Each sample was vertically fixed on the workbench as far as possible with conductive adhesive tape. However, the thickness of Ta coatings could not be directly determined using SEM because the interface between the Ta coating and SLA surface could not be clearly distinguished. To overcome this issue, a reference line was selected, as shown in Figure 2 for both the Ta-coated and uncoated SLA implants. Distance from the surface margin to the reference line of the cross section in the neck area was measured as the thickness. The thickness was measured at 4 sites for each sample (Fig. 3). These 2 sets of data were statistically analyzed, and the difference of these values was the thickness of Ta coatings.

Fig. 1. Photograph of SLA implant before Ta coating. The implants had slightly tapered bodies with an outer diameter of 4 mm and a length of 8 mm. The surface was obtained after SLA treatments. They were designed and manufactured as substrates for the preparation of Ta-coated implants.

Table 1. Vacuum Plasma Spraying Parameters for Preparation of Ta Coatings

Spray Parameters	Numerical Values
Ar gas flow rate (slpm)	40
H_2 gas flow rate (slpm)	10
Spray distance (mm)	270
Pressure (Pa)	10^4
Powder carrier gas (Ar) flow rate (slpm)	2.0
Powder feed rate (g/min)	20
Current (A)	650
Voltage (V)	60

Ta-coated surfaces were fabricated with a spraying distance of 270 mm. Ta powder feed rate was 20 g/min. This spraying process was completed in a vacuum chamber with a low-vacuum pressure of 10^4 Pa.

Another 6 Ta-coated samples were selected, and 3 parts were classified for each sample, including the neck, central, and root area (Fig. 4, A–C). As well, 6 uncoated SLA implants were served as control. These samples were horizontally fixed on the workbench with conductive adhesive tape.

For each part, 4 sites were examined using SEM at ×10.0k magnification. Because of the pitted structures on the surface, some pores buried in these areas were not completely visible. Therefore, the maximum diameter of these pores was difficult to measure. In the same visible field of each site, the sizes of the clearly exposed pores were measured.
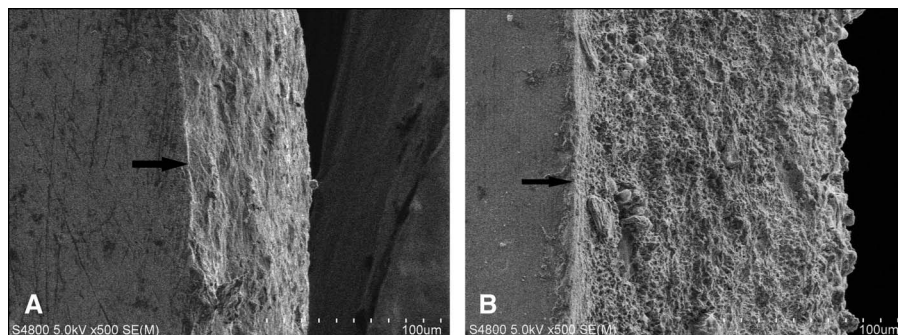
Fig. 2. Black arrow showed the reference line for thickness measurement. Interface between SLA layer and pure Ti substrate was selected as the reference line. (A) It showed the reference line for uncoated SLA implants. (B) It showed the reference line for Ta-coated SLA implants. Distance from the surface margin to the reference line of the cross section in the neck area was measured as the thickness.
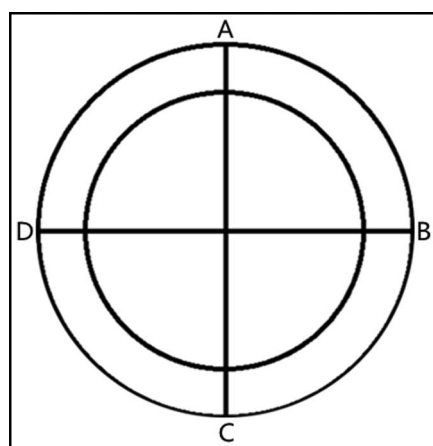
Fig. 3. Schematic diagram showed the selected 4 sites (**A**–**D**) for thickness measurement. They were selected equally from the circular cross section in the neck area of both the Ta-coated and uncoated SLA samples. Then the data obtained were subtracted to determine the thickness of Ta coating.

Statistical Analysis

The data obtained were analyzed using statistical software (SPSS v20.0; IBM, New York, NY). Paired sample t tests were performed to compare the different thicknesses of the different sites. A P value below 0.05 was considered statistically significant. Independent sample t tests were performed to determine the 95% confidence interval (CI) of the difference of the population mean for the thickness of the Ta-coated and uncoated SLA implants. A box plot was made to evaluate the distribution range of the pore size for each part (neck, central, and root).

RESULTS

Ta coating implants were successfully prepared using VPS (Fig. 5), and their microstructure, Ta coating thickness, and pore size were evaluated.

Morphology of Ta Coating Surfaces

The SEM images in Figure 6, A–I show the initial surface morphology of a porous Ta coating prepared using VPS with a spraying distance of 270 mm. Similar to the surface of uncoated SLA implants (Fig. 7, A and B), the surface consisted of a rich pitted

structure and pores of different sizes. No visible surface cracks were observed on the deposited layer (Fig. 8). Moreover, no obvious cracks were observed for the cross section of the Ta-coated samples with mechanical cutting. The interface between the Ta coating and SLA surface was tightly bonded.

Ta Coating Thickness

The thickness at each site was measured for the Ta-coated and uncoated SLA samples (Table 2). The statistical analysis indicated that these 2 sets of data were characterized by normal distributions (Table 3). The results of the paired sample t tests revealed no significant difference between the groups ($P > 0.05$) (Table 4). These 2 sets of data were also analyzed with independent sample t tests. The results indicated that the 95% CI of the difference of the population mean was (114.0759, 129.3574), which was regarded as the 95% CI of the Ta coating thickness.

Pore Size

The pore sizes of Ta coatings and SLA surfaces were determined using SEM at ×10.0k magnification (Fig. 9). The maximum diameter of pores on Ta-coated surface was on the nanoscale. The SEM images revealed that the distribution of the diameter of pores ranged from 40 to 857 nm, which was concentrated at 200 to 400 nm. In addition, the minimum diameter of smaller pores below 40 nm was not distinctly visible for measurement at ×10.0k

Fig. 5. Photograph of the Ta-coated SLA implant. Ta coatings were successfully prepared using VPS. The thread-form structure of the implant surface was still clearly visible.

Fig. 4. Three parts (**A**: neck; **B**: central; **C**: root) were classified for measurement of pore sizes of SLA and Ta-coated samples. (**A**) It is the neck part of the Ta-coated implant. (**B**) It is the central part of the Ta-coated implant. (**C**) It is the root part of Ta-coated implant. For each part, 4 sites were randomly selected and pore sizes of each site were examined using SEM at ×10.0k magnification.
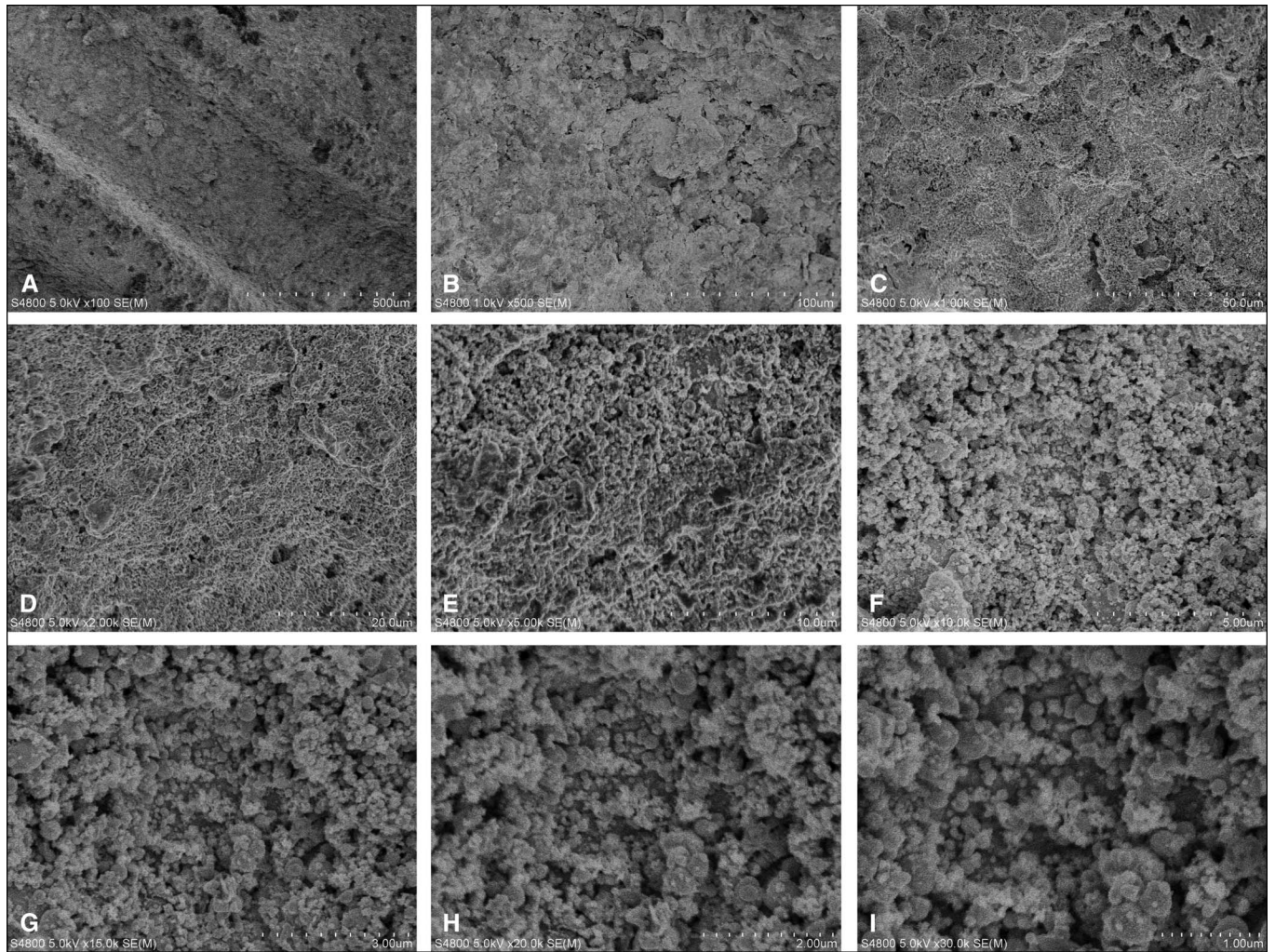
Fig. 6. Initial morphological characteristics of Ta coatings at varying magnifications (without histologic staining) were showed. (**A**) The SLA surface was fully covered by Ta coatings and implant threads were clear (×100 magnification). (**B**) Ta-coated surface was dense and tight (×500k magnification). (**C**) No visible cracks were observed on the Ta-coated surface at ×1.0k magnification. (**D**) SEM image showed circular pitted structure at ×2.0k magnifiction. (**E**) The microstructure of pores was clearly observed (×5.0k magnification). Some pores were buried in these pits. (**F**) Pores on the Ta-coated surface were in a circle-like shape. The maximum diameter of the pores was on the nanoscale (×10.0k magnification). (**G**) It showed the porous structure of Ta coatings at ×15.0k magnification. Pores of various sizes distributed on the Ta coatings and connected with each other. (**H**) SEM image showed a pit with a diameter of 50 μm (×20.0k magnification). (**I**) The pit was nearly in a circular shape and surrounded by pores (×30.0k magnification).
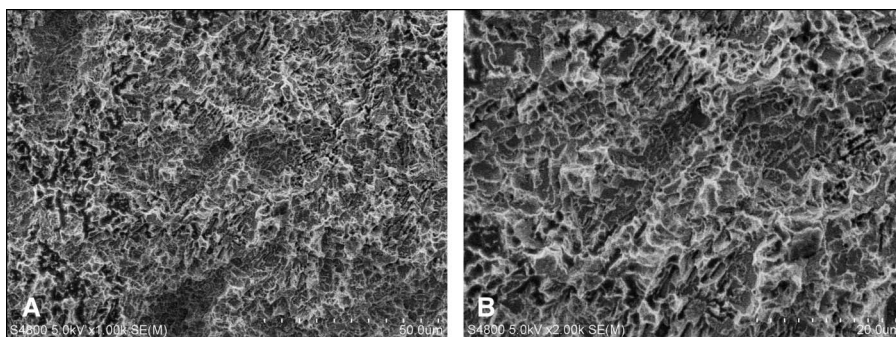
Fig. 7. Initial morphological characteristics of the uncoated SLA implants. (**A**) A multilevel microporous structure could be observed at ×1.00k magnification. The SLA surface was rich of various size pores. (**B**) The pore diameters were examined at ×2.00k magnification. The maximum pore size ranged from 20 to 60 μm and the minimum pore size was from 2 to 6 μm. So the micron-sized Ta particles (5–15 μm) could crystallize between these multiple holes.
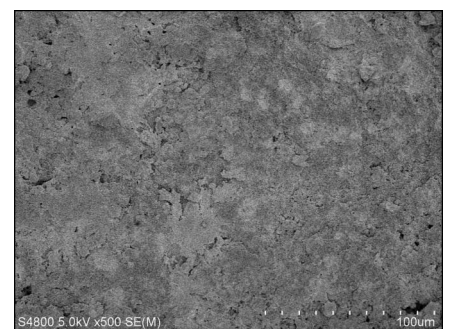
Fig. 8. Surface morphology of Ta coatings at ×500 magnification. No visible cracks were observed on the Ta-coated SLA surface. This indicated a compact structure of Ta coating surface.

Table 2. Surface Thickness of Each Site for Ta-Coated and Uncoated SLA Samples

Samples	SLA (μm)				TaSLA (μm)			
	A	B	C	D	A	B	C	D
1	55.6	53.3	54.5	56.5	191	211	198	206
2	54.5	51.5	54.8	53.2	194	183	173	185
3	50.4	51.6	50.3	49.9	156	158	157	159
4	51.3	53.1	50.6	49.8	155	161	144	148
5	53.4	55.9	52.2	54.7	176	190	187	180
6	49.8	50.5	47.3	52.1	168	169	159	170

The thickness was measured at each site for Ta-coated and uncoated SLA samples using SEM at ×500 magnification. These 2 sets of data were statistically analyzed and the difference of these values was the thickness of Ta coatings.

Table 3. Normality Test (Shapiro–Wilk) for Thickness Data

Samples	N	P
TaSLA	24	0.534
SLA	24	0.621

N, sample size.
Results of Shapiro–Wilk test indicated that these 2 sets of data (thickness of both Ta-coated and uncoated SLA samples) were characterized by normal distributions. So paired sample *t* test can be performed to compare the difference between these 2 groups.

Table 4. Paired Sample *t* Test Was Used to Analyze the Thickness Difference Between 2 Groups

Samples	Pair	N	P
SLA	SLAA—SLAB	5	0.877
	SLAC—SLAD	5	0.325
	SLAA—SLAC	5	0.078
	SLAB—SLAD	5	0.963
TaSLA	TaSLAA—TaSLAB	5	0.282
	TaSLAC—TaSLAD	5	0.143
	TaSLAA—TaSLAC	5	0.492
	TaSLAB—TaSLAD	5	0.186

N, sample size.
The results revealed no statistical significance ($P > 0.05$), suggesting that a uniform coating thickness can be obtained using VPS.
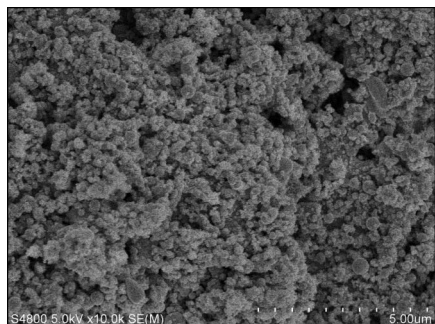
Fig. 9. Measurement of the pore sizes of Ta-coated surface at ×10.0k magnification. Microstructure of VPS Ta-coated surface was examined using SEM. Pore sizes were with a concentrated distribution at 200 to 400 nm on the nanoscale.

magnification. As to the control group, a multilevel microporous structure of uncoated SLA surface could be observed. The maximum pore size ranged from 20 to 60 μm, and the minimum pore size ranged from 2 to 6 μm.

DISCUSSION

Because of their favorable mechanical and biological properties, Ti and its alloys are widely used in implant dentistry. Factors including osseointegration and the amount of bacterial colonization around the implants affect the final outcome of dental treatment.

To achieve an increased survival rate, numerous techniques have been introduced to improve the biological properties of Ti implants. However, inflammation-induced implant loss remains challenging.[27] In the study, Ta was selected for coating Ti implants using VPS. Previous studies have demonstrated the excellent bone ingrowth of porous Ta in orthopedics. Moreover, porous Ta even performed well for a revision surgery for an infected total knee arthroplasty[14] and promoted osseointegration under diabetes conditions.[28] However, little is known about its biological and antibacterial activities in the complex oral cavity. The changing microbiota and pH values in saliva require higher stability and antibacterial activities for the implant surface. This Ta-coated dental implant is expected to be a new form of enhancement for bone formation and antibacterial properties. Moreover, compared with the high cost of manufacturing PTTM,[17] VPS is a much simpler and relatively economical method. The experimental results indicate that Ta-coated implants with porous structures were successfully fabricated using VPS (Fig. 5).

In the experiment, SLA dental implants were used as substrates with cellular morphological surfaces (Fig. 7). The micron-sized Ta particles (5–15 μm) crystallized between multiple holes (2–6 μm, 20–60 μm) on the surface of the SLA implants. Reclaru et al[29] observed that the porous morphology of coatings was affected by the coating process parameters, resulting in different corrosion resistance. By adjusting the experimental spray parameters, rough surfaces rich in pores of different sizes were prepared. No cracks were observed on the Ta coating surface or Ta coating/SLA surface interface. The tightly bonded interface indicates a positive bonding strength between the Ta coating and SLA surface, an important factor for the long-term stability of implants. To further examine the porous structured surface, the thicknesses of the Ta coatings were determined. Statistical analysis revealed no significant difference between the groups, suggesting that a uniform coating thickness can be obtained using the spraying parameters

applied in this work. However, the fixed angle of the samples may result in unavoidable errors. The relationship between the thickness and bonding strength lacks sufficient evidence.

Unlike the SLA surface containing a distribution of micron-sized pores, the Ta coating surface was flatter and consisted of dense nanosized pores. Previous studies revealed normal osteoblastic growth on the surface of nanoporous alumina containing pores with an average diameter of approximately 160 nm.[30] The pores on the Ta coating surface had similar diameters with a concentrated distribution of 200 to 400 nm. Although smaller pores were present, they were ignored because of the measurement difficulty. Alkali-heat-treating of Ti with a nanotopographic surface has been reported to enhance gingival fibroblastic collagen synthesis and result in periodontal-like connective tissue attachment. Moreover, the preparation of a nanocrystalline Ta surface resulted in superior mechanical properties and corrosion resistance compared with coarse-grained Ta.[31] Thus, this nanostructured porous Ta coating surface is expected to be beneficial for bone formation and is expected to perform well in the oral cavity.

CONCLUSION

The feasibility of using VPS to prepare Ta coatings on SLA dental implants was demonstrated in this work. The nanoporous structure of these novel implants may be effective in facilitating osseointegration compared with the structure of uncoated SLA implants. Further studies are needed to analyze the effect of these Ta coatings on biological reactions and antibacterial activity.

DISCLOSURE

The authors claim to have no financial interest, either directly or indirectly, in the products or information listed in the article.

APPROVAL

This article is Part 1. Animal study will be reported in Part II afterward. The experimental animal protocol has been approved by the Biomedical Ethics Committee, Peking University. The approval number is LA2016313.

ROLES/CONTRIBUTIONS BY AUTHORS

X. Zhou: Performed all experiments and contributed to manuscript writing. X. Hu: Contributed to experimental design. Y. Lin: Provided financial support for this study.

REFERENCES

1. Yan Y, Chibowski E, Szcześ A. Surface properties of Ti-6Al-4V alloy part I: Surface roughness and apparent surface free energy. *Mater Sci Eng C Mater Biol Appl.* 2017;70(pt 1):207–215.

2. Novaes A, Papalexiou V, Grisi M, et al. Influence of implant microstructure on the osseointegration of immediate implants placed in periodontally infected sites. A histomorphometric study in dogs. *Clin Oral Implants Res.* 2004;15:34–43.

3. Al-Nawas B, Groetz K, Goetz H, et al. Comparative histomorphometry and resonance frequency analysis of implants with moderately rough surfaces in a loaded animal model. *Clin Oral Implants Res.* 2008;19:1–8.

4. Huang Y, Xiropaidis A, Sorensen R, et al. Bone formation of titanium porous oxide (TiUnite) oral implants in type IV bone. *Clin Oral Implants Res.* 2005;16:105–111.

5. Mendes V, Moineddin R, Davies J. Discrete calcium phosphate nanocrystalline deposition enhances osteoconduction on titanium based implant surfaces. *J Biomed Mater Res A.* 2009;90:577–585.

6. Meng HW, Chien EY, Chien HH. Dental implant bioactive surface modifications and their effects on osseointegration: A review. *Biomark Res.* 2016;4:24.

7. Grischke J, Eberhard J, Stiesch M. Antimicrobial dental implant functionalization strategies -A systematic review. *Dent Mater J.* 2016;35:545–558.

8. Schildhauer TA, Robie B, Muhr G, et al. Bacterial adherence to tantalum versus commonly used orthopedic metallic implant materials. *J Orthop Trauma.* 2006;20:476–484.

9. Alhalawani AM, Mehrvar C, Stone W, et al. A novel tantalum-containing bioglass. Part II. Development of a bioadhesive for sternal fixation and repair. *Mater Sci Eng C Mater Biol Appl.* 2017;71:401–411.

10. Zhu Y, Gu Y, Qiao S, et al. Bacterial and mammalian cells adhesion to tantalum-decorated micro-/nano-structured titanium. *J Biomed Mater Res A.* 2017;105:871–878.

11. Zardiackas LD, Parsell DE, Dillon LD, et al. Structure, metallurgy, and mechanical properties of a porous tantalum foam. *J Biomed Mater Res.* 2001;58:180–187.

12. Matsuno H, Yokoyama A, Watari F, et al. Biocompatibility and osteogenesis of refractory metal implants, titanium, hafnium, niobium, tantalum and rhenium. *Biomaterials.* 2001;22:1253–1262.

13. Stiehler M, Lind M, Mygind T, et al. Morphology, proliferation, and osteogenic differentiation of mesenchymal stem cells cultured on titanium, tantalum, and chromium surfaces. *J Biomed Mater Res A.* 2008;86:448–458.

14. Sambaziotis C, Lovy AJ, Koller KE, et al. Histologic retrieval analysis of a porous tantalum metal implant in an infected primary total knee arthroplasty. *J Arthroplasty.* 2012;27:1413.e5–1413.e9.

15. Bencharit S, Byrd WC, Altarawneh S, et al. Development and applications of porous tantalum trabecular metal-enhanced titanium dental implants. *Clin Implant Dent Relat Res.* 2014;16:817–826.

16. Peron C, Romanos G. Immediate placement and occlusal loading of single-tooth restorations on partially threaded, titanium tantalum combined dental implants: 1-year results. *Int J Periodontics Restorative Dent.* 2016;36:393–399.

17. Sikri N, Kaur M, Lahori M. Tantalum dental implants: An insight. *Guident.* 2016;9:16–19.

18. Liu Y, Bao C, Wismeijer D, et al. The physicochemical/biological properties of porous tantalum and the potential surface modification techniques to improve its clinical application in dental implantology. *Mater Sci Eng C Mater Biol Appl.* 2015;49:323–329.

19. Levine BR, Sporer S, Poggie RA, et al. Experimental and clinical performance of porous tantalum in orthopedic surgery. *Biomaterials*. 2006; 27:4671–4681.

20. Flanigan P, Kshettry VR, Benzel EC. World war II, tantalum, and the evolution of modern cranioplasty technique. *Neurosurg Focus*. 2014;36:E22.

21. Lee GW, Park KS, Kim DY, et al. Results of total hip arthroplasty after core decompression with tantalum rod for osteonecrosis of the femoral head. *Clin Orthop Surg*. 2016;8:38–44.

22. Kaplan RB. Open cell tantalum structures for cancellous bone implants and cell and tissue structures. 1994. U.S. Patent No. 5282861.

23. Cohen R. A porous tantalum trabecular metal: Basic science. *Am J Orthop (Belle Mead NJ)*. 2002;31: 216–217.

24. Kim DG, Huja SS, Tee BC, et al. Bone ingrowth and initial stability of titanium and porous tantalum dental implants: A pilot canine study. *Implant Dent*. 2013;22:399–405.

25. Tang Z, Xie Y, Yang F, et al. Porous tantalum coatings prepared by vacuum plasma spraying enhance BMSCS osteogenic differentiation and bone regeneration in vitro and in vivo. *PLoS One*. 2013;8:e66263.

26. Guimond-Lischer S, Ren Q, Braissant O, et al. Vacuum plasma sprayed coatings using ionic silver doped hydroxyapatite powder to prevent bacterial infection of bone implants. *Biointerphases*. 2016;11:011–012.

27. Charalampakis G, Leonhardt A, Rabe P, et al. Clinical and microbiological characteristics of peri-implantitis cases: A retrospective multicentre study. *Clin Oral Implants Res*. 2012;23:1045–1054.

28. Wang L, Hu X, Ma X, et al. Promotion of osseointegration under diabetic conditions by tantalum coating-based surface modification on 3-dimensional printed porous titanium implants. *Colloids Surf B Biointerfaces*. 2016;148: 440–452.

29. Reclaru L, Eschler PY, Lerf R, et al. Electrochemical corrosion and metal ion release from Co-Cr-Mo prosthesis with titanium plasma spray coating. *Biomaterials*. 2005;26:4747–4756.

30. Briggs EP, Walpole AR, Wilshaw PR, et al. Formation of highly adherent nano-porous alumina on Ti-based substrates: A novel bone implant coating. *J Mater Sci Mater Med*. 2004;15: 1021–1029.

31. Huo WT, Zhao LZ, Yu S, et al. Significantly enhanced osteoblast response to nano-grained pure tantalum. *Sci Rep*. 2017;7:40868.